Noninvasive fluorescence excitation spectroscopy for the diagnosis of oral neoplasia *in vivo*

Jeyasingh Ebenezar
Singaravelu Ganesan
Prakasarao Aruna
Radhakrishnan Muralinaidu
Kannan Renganathan
Thillai Rajasekaran Saraswathy

SPIE

Noninvasive fluorescence excitation spectroscopy for the diagnosis of oral neoplasia *in vivo*

Jeyasingh Ebenezar,[a*] **Singaravelu Ganesan,**[a] **Prakasarao Aruna,**[a] **Radhakrishnan Muralinaidu,**[b] **Kannan Renganathan,**[b] **and Thillai Rajasekaran Saraswathy**[b]
[a]Anna University, Department of Medical Physics, Chennai 600025, India
[b]Ragas Dental College, Department of Oral & Maxillofacial Pathology, Chennai 600096, India

Abstract. Fluorescence excitation spectroscopy (FES) is an emerging approach to cancer detection. The goal of this pilot study is to evaluate the diagnostic potential of FES technique for the detection and characterization of normal and cancerous oral lesions *in vivo*. Fluorescence excitation (FE) spectra from oral mucosa were recorded in the spectral range of 340 to 600 nm at 635 nm emission using a fiberoptic probe spectrofluorometer to obtain spectra from the buccal mucosa of 30 sites of 15 healthy volunteers and 15 sites of 10 cancerous patients. Significant FE spectral differences were observed between normal and well differentiated squamous cell carcinoma (WDSCC) oral lesions. The FE spectra of healthy volunteers consists of a broad emission band around 440 to 470 nm, whereas in WDSCC lesions, a new primary peak was seen at 410 nm with secondary peaks observed at 505, 540, and 580 nm due to the accumulation of porphyrins in oral lesions. The FE spectral bands of the WDSCC lesions resemble the typical absorption spectra of a porphyrin. Three potential ratios (I_{410}/I_{505}, I_{410}/I_{540}, and I_{410}/I_{580}) were calculated from the FE spectra and used as input variables for a stepwise linear discriminant analysis (SLDA) for normal and WDSCC groups. Leave-one-out (LOO) method of cross-validation was performed to check the reliability on spectral data for tissue characterization. The diagnostic sensitivity and specificity were determined for normal and WDSCC lesions from the scatter plot of the discriminant function scores. It was observed that diagnostic algorithm based on discriminant function scores obtained by SLDA–LOO method was able to distinguish WDSCC from normal lesions with a sensitivity of 100% and specificity of 100%. Results of the pilot study demonstrate that the FE spectral changes due to porphyrin have a good diagnostic potential; therefore, porphyrin can be used as a native tumor marker. © *2012 Society of Photo-Optical Instrumentation Engineers (SPIE).* [DOI: 10.1117/1.JBO.17.9.097007]

Keywords: fluorescence excitation spectra; discriminant function scores; oral lesions; porphyrin; spectral intesity ratio parameters; stepwise linear discriminant analysis; squamous cell carcinoma.

Paper 12302 received May 18, 2012; revised manuscript received Aug. 17, 2012; accepted for publication Aug. 23, 2012; published online Sep. 21, 2012.

1 Introduction

Oral cavity cancer is a major health concern all over the world. India has one of the highest incidences of oral cancer in the world, and it ranks first in males and third in females.[1,2] This is primarily associated with the habit of betel quid chewing, pan, and tobacco usage of large population in India. In spite of advancements in the field of cancer detection and therapy, the 5-year survival rate of oral cancer patients is still below 60%. Progression from premalignant to cancerous condition takes place usually over many years, which can be prevented if detected in its formative stages. The delay in diagnosis may be partly due to the ignorance of public about the symptoms of oral precancer and the need for routine oral cancer screening. Proper management of patients with benign, premalignant or malignant oral lesion often starts with its accurate diagnosis. Biopsy followed by histopathology is the gold standard technique for oral cancer screening. However, biopsy is painful, and pathological analysis is time consuming and error prompt due to manual or sampling mistakes. Moreover,

by the time the patient reaches the clinic for a biopsy followed by histopathological evaluation, the disease would have progressed beyond the treatment stage in most cases. Hence, alternative noninvasive methods that can provide molecular level information needs to be looked into for effective intervention for the management of oral cancer.

Tissue diagnosis using optical spectroscopy has been considered an alternative to the conventional diagnostic methods because of its advantages such as minimal invasiveness, simplicity in recording, minimal time required for the study, comfort to the patients, and reproducibility.[3–7] Further, optical spectroscopy has the potential to detect malignant lesions earlier, before they become macroscopically visible, by probing tissue biochemistry and morphology *in vivo* real time. In this regard, various optical spectroscopic techniques such as autofluorescence fluorescence spectroscopy (AF),[8–20] diffuse reflectance spectroscopy (DRS),[21–23] and Raman spectroscopy (RS)[24] are the emerging *in vivo* diagnostic tools for cancer.

However, fluorophores, absorbers, and scatters present in tissue allow one to obtain biochemical, structural and molecular information through AF, DRS, and RS for the diagnosis procedure in oral oncology. For example, AF spectroscopy provides information about the endogenous tissue fluorophores excited with suitable wavelength of excitation. The presence of disease

*Present address: PG & Research Department of Physics, Jamal Mohamed College (Autonomous), Tiruchirappalli 620020, India.

Address all correspondence to: Ebenezar Jeyasingh, Anna University, Department of Medical Physics, Chennai 600025, India; Tel: 91 9865007640; Fax: 91-44-222352270; E-mail: ebey_ebenezar@yahoo.com; Singaravelu Ganesan, E-mail: sganesan@annauniv.edu

changes the concentration of these fluorophores, which makes spectral features sensitive to tissue alterations. The DRS gives information about tissue absorbers and scatters, which are believed to change with tissue transformation. The RS provides spectrally narrow and well defined signatures, which can be related to the structure of specific molecular groups in a sample for tissue diagnosis. Since these three spectroscopic modalities provide complimentary information about tissue compositions, their combination should provide useful information about tissue status.

Tissues are highly heterogeneous with many intrinsic fluorophores such as tryptophan, tyrosine, phenylalanine, collagen, elastin, reduced form of nicotinamide adenine dinucleotide (NADH), flavin adenine dinucleotide (FAD), and endogenous porphyrins. Each fluorophores has a characteristic wavelength for excitation with an associated characteristic emission.[25] Nevertheless, fluorescence emission/excitation spectroscopy, emission spectra at one or more excitation wavelengths or excitation spectra corresponding to one or more emission wavelengths have been used for diagnostic purpose.[26] In general, fluorescence emission spectroscopy is used to measure the emission properties fluorophores, while fluorescence excitation spectroscopy provides information about the absorption characteristics of fluorophores.

In addition to the conventional fluorescence emission spectroscopy, fluorescence excitation spectroscopy (FES) is a complementary technique, which is dependent on the absorption properties of the fluorophores used as a potential tool for the diagnostic purposes.[27–29] In this technique, the signal is recorded by keeping the peak emission wavelength of the fluorophore of interest to be fixed for excitation and the corresponding intensity of fluorophore absorption characteristics to be measured. Alfano et al. first demonstrated the potential use of FES as a diagnostic tool for the discrimination of malignant from benign breast tissues.[27] Kollias et al. investigated *in vivo* on normal human volunteers as well as on patients with psoriasis and it was found that characteristics excitation band of specific skin fluorophores was identified.[28] Moan et al. evaluated that FE spectra of PpIX used for the assessment of penetration depths of 5-aminolevulinic acid after topical application in normal mouse skin.[29] The above cited reports suggest that FES may be used to detect and evaluate the absorbing characteristics of fluorophores in normal and different pathologically transformed tissues.

Although many extensive studies were made in the characterization and detection of cancer using various optical spectroscopy techniques, to the best of our knowledge, there are no reports of *in vivo* studies on the FES technique in the characterization and discrimination of normal from cancerous oral subjects. In this context, the focus of the study was on the *in vivo* characterization of healthy and oral cancerous patients using FES technique. The efficacy of the FE spectral intensity ratios in discrimination of well differentiated squamous cell carcinoma (WDSCC) from normal lesions with their statistical significance was verified by stepwise linear discriminant analysis (SLDA) and the results were presented.

2 Materials and Methods

2.1 Study Population

The present study consisted of 15 healthy volunteers maintaining good oral hygiene and no habit of chewing betel nut or tobacco. The healthy volunteers were students (9 men and 6 women) within the age group of 20 to 30 years, with a mean age of 27 years. Fluorescence excitation (FE) spectra were acquired from two sites (left and right buccal mucosa) of the each healthy volunteer. Like that, 30 sites were measured from 15 healthy volunteers. Ten patients with confirmed squamous cell carcinoma of either right or left buccal mucosa were included in this study. The FE spectra from 15 sites with a clinically observable lesion were acquired from 10 cancerous patients (6 men and 4 women) within the age group of 40 to 60 years, with a mean age of 52 years. All the patients included in this study had prolonged habits of chewing either betel quid or processed areca nut or both chewing and smoking simultaneously or alcohol consumption. An experienced dental surgeon identified suspicious lesions in the left or right buccal mucosal site where the fiberoptic probe was gently placed for spectral measurements. The study was approved by the ethics committee of Ragas Dental College, Chennai. The procedure, reassurance, and counseling were given to the healthy volunteers and cancerous patients, and their consent letter in the regional language was obtained before the measurements.

2.2 Study Protocols

Before recording the spectra, all the volunteers and cancerous patients were asked to rinse their mouth for 1 min with saline solution in order to avoid the presence of food or any other intake that they recently consumed. After completion of *in vivo* FE spectral measurements from suspicious sites from the cancerous patients, a biopsy (2×2 mm^2 approximately in size) was taken from the measurement sites and sent for histopathological analysis after fixing in 10% formalin solution. The biopsy slides were prepared and classified by an experienced oral pathologist, who was blinded to the FE spectral results. In the case of healthy volunteers, instead of biopsy, visual impression was carried out by the dental surgeon. After classification, spectroscopic data were correlated with the histopathological findings.

2.3 Instrumentation

In vivo FE spectra were obtained from buccal mucosal site of the cancerous patients and each normal left and right buccal mucosal site of the healthy volunteers using a hand-held optical fiber probe attached to Fluoromax-2 spectrofluorometer (ISA Jobin Yvon-Spex, Edison, NJ) schematic instrumentation diagram is shown in Fig. 1. The excitation source (150 W ozone-free xenon arc lamp) coupled to the excitation monochromator delivers light to the sample spot at a desired wavelength, and the fluorescence emission from the tissues is collected by another emission monochromator connected to a photomultiplier tube (R928P, Hamamatzu, Shizuoka-Ken, Japan). The desired excitation wavelength and the emission wavelength were selected by a personal computer (PC), which controlled the monochromators. For *in vivo* applications, the excitation light was guided to illuminate buccal mucosal site by one arm of a Y-type quartz fiber bundle, and the emission fluorescence was collected by another arm of the fiber bundle and directed to the photomultiplier detector. The collected fluorescence signal was then amplified and transferred signal was displayed on the PC monitor through an RS232 interface. The data were processed by the Windows-based data acquisition program Data Max powered by GRAMS/386. All Fluoromax-2 functions are controlled by Data
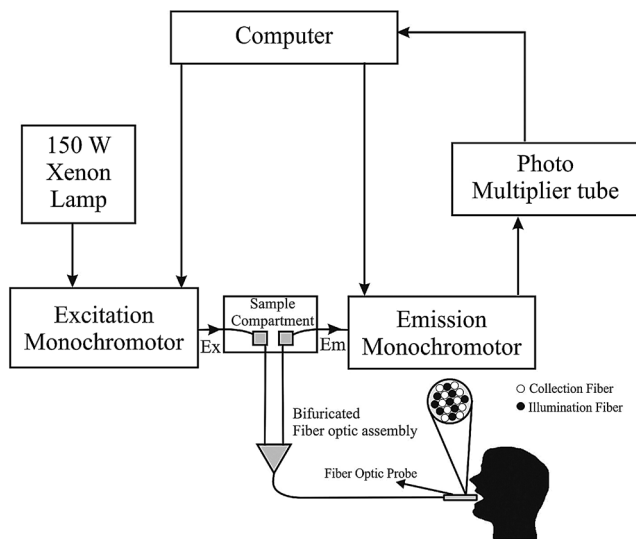
Fig. 1 Schematic diagram showing the experimental set up for *in vivo* FE spectral measurements. The Ex and E_m represent the direction of excitation and emission light.

Max software (Dover corporation NYSE:DOV, Orlando, FL), which communicates between a PC-compatible computer and the Fluoromax-2. In the *in vivo* measurements, a bifurcated randomized fiber optic bundle of model 1950M is used with the fiber optic platform of model 1950F (Fig. 1).

2.4 FE Spectral Data Acquisition

The instrument was turned on 30 min before the measurements were taken in order to improve stability and reduce noise. The variation in the excitation light source intensity was accounted for by dividing the measured spectrum with the reference signal from the excitation light source. Prior to start of each measurement day, a background spectrum was obtained at excitation wavelength by inserting the probe into a nonfluorescent bottle filled with distilled water. The background spectrum was then subtracted from the corresponding tissue FE spectrum.

During the FE spectral measurements, the desired peak emission wavelength is fixed for the emission monochromator and the corresponding fluorescence excitation intensity range to be recorded in the excitation monochromator. The FE spectral measurements were recorded between 340 and 600 nm excitation wavelengths for an emission wavelength of 635 nm, for which the excitation and the emission wavelength band passes were set at 5 nm and 3 nm respectively, with an integration time of 0.1 s. In the present study, the emission wavelength of 635 nm is selected because it represents a porphyrin emission maximum and hence the corresponding fluorescence excitation spectra were recorded between 340 and 600 nm in 1 nm increments. The gratings in the excitation and emission monochromators have a groove density of 1200 grooves/mm and are blazed at 330 and 500 nm, respectively.

The fiber optic probe had a numerical aperture of 0.22 and was approximately 0.9 mm in outer diameter (used for the *in vivo* measurements) contained 31 delivery and 31 collection fibers of 250 μm diameter randomly mixed. The optical fiber probe was disinfected with 2.4% gluteraldehyde solution, rinsed with phosphate buffered-saline. The distal end of the probe was

covered with a flexible spacer (sleeve) 1 cm long, made of black polyvinal chloride (PVC), which maintains a fixed separation of approximately 0.5 cm between the probe tip and tissue surface and maximizes the fluorescence signal by providing optimum overlap between the excitation and collection areas. Since this opaque sleeve is disposable, it provides extra hygiene and it also protects the fiber tips from contamination by oral cavity saliva. The FE spectra were recorded with the PVC sleeve (tip) of the fiber optic probe was gently touched on the surface of the healthy and cancerous buccal mucosal sites.

2.5 Data Processing and Statistical Analysis

The FE spectral data recorded from buccal mucosal sites of patients and volunteers were categorized into two groups based on pathological reports as normal ($n = 30$) from 15 healthy volunteers, and cancerous lesions ($n = 15$) from 10 patients.

Detailed statistical analysis of the data sets for normal, and cancerous oral lesions was carried out. This involved the following four primary steps: 1. normalization of each FE spectrum; 2. identifying characteristic spectral features from the experimental group and introducing different spectral intensity ratio parameters; 3. statistical verification of ratio parameters using unpaired student's *t*-test; and 4. development of a classification algorithm using SLDA by including the ratio parameters as input variables.

2.5.1 Normalization

Each fluorescence excitation spectrum was normalized by dividing the fluorescence excitation intensity at each emission wavelength by the maximum excitation intensity of the spectrum.

2.5.2 Mean FE spectrum and normalized mean FE spectrum

Mean FE spectra obtained from normal ($n = 30$) and WDSCC ($n = 15$) lesions were averaged separately. Subsequently, each FE spectrum of normal ($n = 30$) and WDSCC ($n = 15$) lesions was normalized individually. The normalized spectral data of both normal and WDSCC were averaged and a normalized mean FE spectrum was obtained.

2.5.3 FE spectral intensity ratios

In order to verify the diagnostic potentiality of these observed spectral signatures between normal and WDSCC oral lesions, three ratio parameters I_{410}/I_{505}, I_{410}/I_{540}, and I_{410}/I_{580} for FE spectra at 635 nm emission were generated. These ratio parameters were selected using fluorescence intensities at those emission wavelengths, which represent the different peaks in the FE spectrum of the cancerous subjects studied.

2.5.4 Student's t-test

The mean and standard deviation values were calculated for all three spectral intensity ratio parameters of I_{410}/I_{505}, I_{410}/I_{540}, and I_{410}/I_{580} between normal and cancerous oral subjects, and their statistical significance was verified using unpaired student's *t*-test to calculate the level of physical significance (p) with 95% confidence interval using origin statistical software (OriginPro7).

2.5.5 *Stepwise linear discriminant analysis*

The SLDA were performed using SPSS/PC + 11.0 statistical software.[30,31] The discriminant analysis used a partial F-test (F to enter 3.84; F to remove 2.71) and a stepwise method (maximum number of steps = 6) to sequentially incorporate the set of 3 variables into a Fisher linear discriminant function. Linear discriminant function is a latent variable, which is created as a linear combination of discriminating variables, such that $L = b_1v_1 + b_2v_2 + \ldots + b_nv_n + c$, where the b's are discriminant coefficients whose values are estimated using discriminating analysis, the v's are discriminating independent ratio variables used for predicting discriminating score, and c is a constant. The linear discriminant function transforms each ratio variable of the sample into a single discriminant score. The discriminant scores obtained through discriminant function analysis is used for tissue classifications. In stepwise discriminant function analysis, a model of discrimination is built step-by-step. Specifically, at each step, all variables are reviewed and evaluated to determine the one that will contribute most to the discrimination between groups. The most significant contributing variable in a discriminant function depends on the order in which the variables appear in the function. The classification function of each group (original grouped cases) could discriminate only that group from the rest of the groups in the analysis. To check the reliability of our analysis, leave-one-out (LOO) method of cross-validation was performed. In this procedure, discriminant scores of one particular sample were eliminated and discriminant analysis was to form a classification algorithm using the remaining samples. The resulting algorithm was then used to classify the excluded case. This process was repeated for each sample (cross-validated grouped cases). This process known as LOO cross-validation or jackknife cross-validation provided optimal use of a small data set to validate the performance of a decision surface without bias.[32] The classification sensitivity and specificity were assessed from the scatter plot of the discriminant function scores by comparison with histopathological results.

3 Results

3.1 *FE Spectral Features*

Figure 2 shows the mean FE spectra from 15 sets ($n = 30$) of spectral measurements taken from the left and right buccal squamous epithelium of 15 healthy volunteers and from 15 sites in 10 WDSCC lesions. It can be seen in Fig. 2(a), the intensity of normal mucosa decreased monotonically with the increase in the wavelength over the entire wavelength range of measurement. Also, it is observed that the normal oral epithelium shows a relatively lesser intensity than WDSCC lesions. Figure 2(b) shows the normalized mean FE spectra of normal and WDSCC lesions. In this spectra, normal tissues shows two sharp spectral peaks at 363 and 388 nm and a broad excitation band around 440 to 470 nm. However, the excitation spectra of WDSCC lesions displayed a spectral profile with four distinct bands centred at around 410, 505, 540, and 580 nm. But these bands were completely absent in the case of normal subjects. In addition, a spectral valley was also observed around 450 to 475 nm for WDSCC lesions.

3.2 *FE Spectral Measurements of Porphyrin Standard Fluorophore*

To investigate the origin of the observed excitation spectral peaks from normal and cancerous oral lesions and to assign
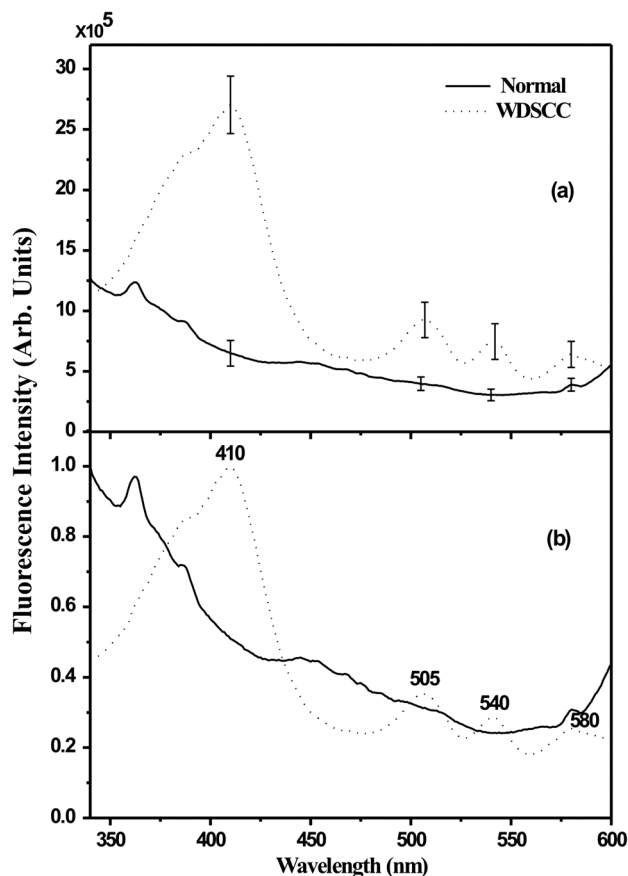

Fig. 2 Normal FE spectral features show the mean of 30 spectral measurements taken from the left and right buccal mucosa of 15 healthy volunteers, whereas the WDSCC FE spectral features represent the mean of 15 spectral measurements from 10 cancerous buccal mucosa patients. (a) Mean FE spectra of normal and WDSCC groups with error bars relate to the standard deviations at 410, 505, 540 and 580 nm. (b) Normalized mean FE spectra of normal and WDSCC groups.

them to appropriate endogenous fluorophores, the FE spectra of commercially obtained fluorophore of porphyrin (Sigma Chemicals, USA) were measured with the same experimental parameters maintained as for the oral lesions. A porphyrin dissolved in methanol was made as a solution and their FE spectrum was measured at 635 nm emission, since the peak emission wavelength of porphyrin is 635 nm. The FE spectrum of the porphyrin was normalized with respect to the corresponding maximum fluorescence intensity. Figure 3 shows the normalized FE spectra of the standard fluorophore of porphyrin has soret band at 411 nm and three Q-bands of absorption observed at 503, 536, and 572 nm.

3.3 *Results of Histological Evaluation*

In the case of healthy volunteers, instead of biopsy, visual inspection was carried out. All the 30 sites measured from 15 healthy volunteers were diagnosed clinically as normal, whereas 15 sites measured from 10 cancerous patients were pathologically diagnosed as WDSCC. The photograph of a 52-year-old male patient was clinically visible on the left buccal mucosa lesion showing ulcero proliferative growth in the left buccal mucosa [Fig. 4(a)]. Histopathological analysis of the
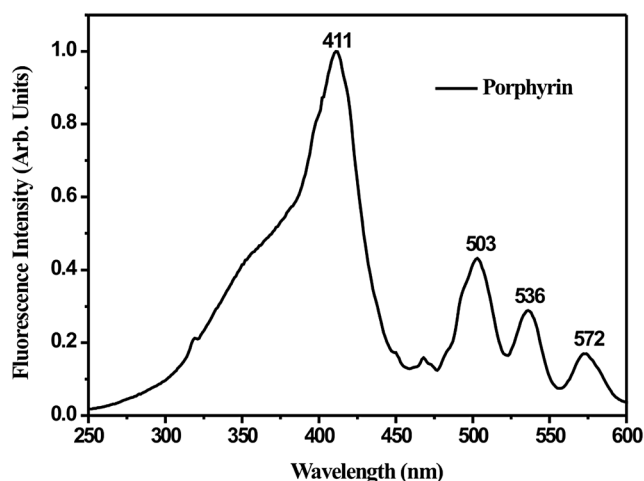
Fig. 3 Normalized FE spectrum of porphyrin standard fluorophore.

biopsied sample from this site shows that it is the case of WDSCC. The histological picture clearly shows the formation of keratin pearls [Fig. 4(b)].

3.4 Results of Statistical Analysis

Mean FE spectral intensity ratios (I_{410}/I_{505}, I_{410}/I_{540}, and I_{410}/I_{580}) determined from the oral mucosal spectra of WDSCC ($n = 15$) lesions from 10 cancerous patients and normal mucosal spectra ($n = 30$) from 15 healthy volunteers are given in Table 1. An unpaired Student's t-test was performed all the 3 FE spectral intensity ratios between normal and WDSCC lesions to determine the statistical significance of the intensity ratio method in differentiating mucosal variations. The results of the mean and standard deviation of the FE spectral ratios of normal and WDSCC lesions were listed in Table 1 along with p values. The p values of the all the three ratio variables are less than 0.001 indicating a high statistical significance. From Table 1, the ratio variables $R_1 = I_{410}/I_{505}$, $R_2 = I_{410}/I_{540}$, and $R_3 = I_{410}/I_{580}$ have found the mean value of the normal tissue to be lower than that of the WDSCC lesions. For example, the mean ratio value of R_1 in normal lesions was 1.63 ± 0.16, which is significantly different from the mean value of 3.09 ± 0.24 in WDSCC lesions (Unpaired Student's t-test, $p < 0.001$). Similarly, the mean ratio value of R_2 for normal tissue was 2.13 ± 0.23, which is also significantly different from the mean value of 3.93 ± 0.33 for WDSCC tissues (Unpaired Student's t-test, $p < 0.001$). Finally, the mean ratio value of R_2 for normal tissue was 1.67 ± 0.17, which is also significantly different from the mean value of 4.75 ± 0.78 for WDSCC tissues (Unpaired Student's t-test, $p < 0.001$).

3.5 Results of SLDA

Since the present study aims to discriminate between normal and WDSCC oral lesions, the stepwise discriminant analysis were performed across two groups, (i.e.,) normal ($n = 30$) and the WDSCC ($n = 15$) oral lesions resulted in the following expression for a canonical discriminant function (DF):
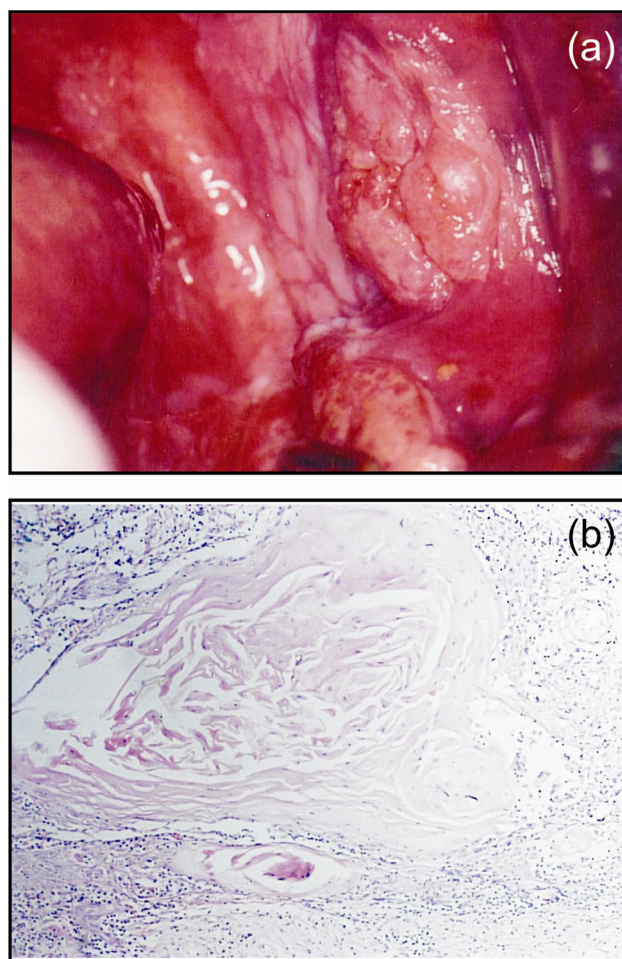

Fig. 4 Photograph of a representative typical cancerous buccal mucosa lesion and their corresponding histolgical view. (a) Clinical picture showing ulcero proliferative growth in the left buccal mucosa (b) Pathological investigation shows WDSCC under $10 \times$ magnification.

$$DF = 5.16R_1 - 10.96.$$

In this analysis, out of the three input ratio variables (R_1, R_2, & R_3), only one ratio variable (R_1) turned out to be significant and it was included in the linear discriminant function. Figure 5 shows the scatter plot of the discriminant function scores of normal and WDSCC individuals. This discriminant function classified the original and the cross-validated grouped cases with a specificity of 100% and sensitivity of 100%. The overall classification accuracy was 100% for both original and

Table 1 Mean $\pm$ SD of the FE spectral intensity ratios of normal and WDSCC oral lesions and their statistical significance (p) was computed through unpaired student's t-test.

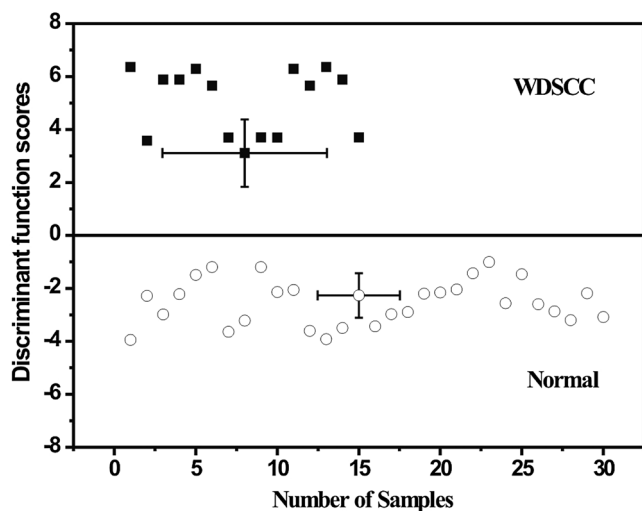| Tissue types	Intensity ratio $R_1 = I_{410}/I_{505}$	Intensity ratio $R_2 = I_{410}/I_{540}$	Intensity ratio $R_3 = I_{410}/I_{580}$
Normal	1.63 ± 0.16	2.13 ± 0.23	1.67 ± 0.17
WDSCC	3.09 ± 0.24	3.93 ± 0.33	4.75 ± 0.78
p value	<0.001	<0.001	<0.001

Fig. 5 Discriminant function scatter plot of normal (○) and WDSCC (■) lesions. The group centroids and the error bars showing the standard deviations.

Table 2 Classification results of the SLDA done across normal versus WDSCC group. Bold figures represent the specificity/sensitivity value of the corresponding group. The total percentage of correctly classified cases gives the average of the percentage of the predicted groups.

Discriminant analysis	Cases	Predicted group membership (%)		Total % of correctly classified cases
		Normal	WDSCC	
I	Original	**100.0**	0.0	100.0
		0.0	**100.0**	
	Cross-validated	**100.0**	0.0	100.0
		0.0	**100.0**	

cross-validated grouped cases (Table 2). The group centroids and the error bars showing the standard deviations are also shown in the Fig. 5. The results of the classification analysis are given in Table 2.

4 Discussion

The potential use of FES technique in detection and characterization of normal and WDSCC oral tissues was explored, and the spectral data were analyzed by discriminant analysis to validate the diagnostic potentiality of the current method and the results are presented. The comparison of FE spectra of normal and WDSCC oral tissues with those corresponding to commercial grade standard fluorophore of porphyrin suggest that the narrow primary excitation band at 410 nm and three secondary bands at 505, 540, and 580 nm may be attributed to absorptions of soret and Q-bands, respectively. In this study, the wavelengths of the spectral bands observed from WDSCC oral tissues were not exactly the same as those of the standard fluorophore. This observed spectral shift of the peak positions in the spectra of oral tissues may be due to the different microenvironments of these endogenous fluorophores in tissues.

Distinct salient differences in the FE spectral signatures between normal and WDSCC oral lesions were observed. As we had noted earlier, normal lesions exhibits two sharp spectral peaks were observed at 363 and 388 nm due to Rayleigh scattering effect and stray light contribution from the excitation light. A shoulder observed around 440 to 470 nm in the case of normal subjects may be attributed to absorption band of FAD. However, the mean WDSCC lesions revealed a prominent primary band at 410 nm and three secondary spectral bands around 505, 540, and 580 nm, respectively. These bands were completely absent in the case of normal oral lesions. The band around 410 nm is predominant when compared with the other bands. These observed primary and secondary bands correspond to soret and Q-band absorption of endogenous porphyrins, respectively.[25,29,33,34] Further, this observed spectral signature of the malignant lesions resembles the typical absorption spectra of the porphyrin molecule, since it is well known that the malignant tissues are known to accumulate and retain

more porphyrin. Hence, the observed soret and Q-bands spectral signature indicate the presence of endogenous porphyrins synthesized in WDSCC lesions. The specific and excessive accumulation of endogenous porphyrin in tumor tissues is not fully settled. This has been variously attributed to microbial synthesis,[7,9,11,35,36] degradation of hemoglobin,[33] or accumulation of protoporphyrin IX due to lack of ferrochelatase in tumor cells.[8,17,18,37,38] Although there is a controversy concerning the origin of endogenous porphyrin, it is still considered to be one of the important tumor markers in the characterization of tissues.[7–9,17,18,33–37] This observation strongly supports the belief that definite biochemical and morphological changes occurred during the tissue transformation process, which consequently modify this spectroscopic signature of the tissue condition.

Tissue morphology affects fluorescence via absorption and scattering properties of excitation and emission signals. The morphological changes that accompany neoplastic progression also affect the absorption and scattering properties of the tissue which in turn modify the measured signal.[15] Accordingly, the observed FE spectral features have a distinct valley around 450 to 475 nm for WDSCC tissues, which may be attributed to hemoglobin absorption and it could be well appreciated from the normalized mean FE spectra shown in Fig. 2(b). This valley was completely absent in the case of normal tissues, but in its place, a shoulder was observed due to FAD. Cancerous tissues are associated with increased neovasculature due to angiogenesis and hence, increased blood volume might result in reduced fluorescence signal.[22,23] The other contributing factors to this reduction in intensity of light are the breakdown of collagen crosslinks in the stroma, loss of fluorophores such as NADH and FAD, increased epithelial scattering, loss of keratin in the epithelium, and increased hemoglobin absorption associated with increased microvascular density throughout the epithelial-stromal region.[7,38,39]

The SLDA using spectral intensity ratio variables has been performed by many groups for spectral analysis and it could be used for potential tool for tissue diagnosis.[30,31,40] In the present study, a simple classification method was adopted based on the ratio values estimated from the intensities at different wavelengths characterizing the peaks of WDSCC lesions under study. To quantify the observed spectral results and to estimate the diagnostic potentiality of the present technique, three intensity ratios such as I_{410}/I_{505}, I_{410}/I_{540}, and I_{410}/I_{580} were selected. Each emission wavelength used in these ratios represents specific fingerprint of one emission band. For example, the component identified as I_{410} represents the peak emission

wavelength of soret band, whereas I_{505}, I_{540}, and I_{580} represent the peak emission wavelength of Q-bands of absorption. All the three intensity ratio values increase significantly for WDSCC tissues in comparison with normal tissues. Though these ratio parameters represent the characteristic spectral features and provide useful diagnostic information with excellent discrimination of mean ratio values between normal and WDSCC groups, the classification accuracy of all the 45 samples were not tested in unbiased manner. In order to quantify an unbiased evaluation of the data, cross-validation is required for an accurate estimation of the FES for oral tissue diagnosis. Hence, we pooled the whole set of three ratios and used them as input variables in a SLDA, using SPSS/PC+ as stated earlier.

In this study, the SLDA for three ratio parameters was performed in order to find the sensitivity and specificity of the present technique to discriminate between WDSCC from normal oral lesions. Figure 5 shows the scatter plot of the discriminant function scores from 45 samples are categorized as normal ($n = 30$) and WDSCC ($n = 15$) subjects. The present classification analysis shows that WDSCC tissues are discriminated with a sensitivity of 100%, whereas the specificity to detect normal is 100%. In this discriminant analysis, 100% of both original and cross-validated grouped cases are correctly classified (Table 2, Fig. 5). Since the increased value of the FE spectral intensity ratios of I_{410}/I_{505}, I_{410}/I_{540}, and I_{410}/I_{580} for WDSCC oral lesions compared with normal tissue reflects an accumulation and/or elevation of porphyrin content when normal tissues transformed into cancerous conditions. Note that these excitation peaks were absent in the case of normal lesions, which confirms that definite biochemical and morphological features were occurred in the WDSCC lesions.

Previous works show promising results and excellent diagnostic algorithm developed to diagnose oral precancer based on fluorescence spectra acquired at single and/or multiple excitation wavelengths with combination of one or more technique to improve the diagnostic accuracy.[7–24] As a preliminary investigation, we have studied a few cases in normal and WDSCC group. Although excellent discrimination results were obtained using FES, the hyperplasia and dysplasia lesions were not included in this study. To improve upon the diagnostic capability of FES method, a large population of precancerous and cancerous lesions would be necessary. Such investigations are required to develop classification algorithms for discriminating dysplastic lesions as mild, moderate, and severe, and SCC lesions as well differentiated, moderately differentiated and poorly differentiated, and enhance the potential of FES technique. Currently, we are working on these aspects to prove FES as a useful and novel technique in the diagnostic oncology.

5 Conclusion

The clinical study presented here demonstrates the ability of *in vivo* FES technique to distinguish normal and WDSCC oral lesions. The result of the current study reveals that spectral changes due to porphyrins have good diagnostic potential. Three ratio variables were empirically selected and then evaluated by SLDA. Our results have shown that the FES technique is able to distinguish normal from WDSCC tissues with a specificity of 100%, with corresponding sensitivity of 100%. Our pilot study can also be considered as a complementary method to analyze the key absorption characteristics of fluorophore bands, which can be used as tumor markers for oral cancer detection.

References

1. G. S. Hamada et al., "Comparative epidemiology of oral cancer in Brazil & India," *Tokai J. Exp. Clin. Med.* **16**(1), 63–72 (1991).
2. R. Sankaranarayanan, "Oral caner in India: An epidemiologic and clinical review," *Oral Surg. Oral Med. Oral Path.* **69**(3), 325–330 (1990).
3. R. R. Alfano et al., "Laser induced fluorescence spectroscopy from native cancerous and normal tissues," *IEEE J. Quantum Electron.* **20**(12), 1507–1511 (1984).
4. R. R. Alfano et al., "Fluorescence spectra from cancerous and normal human breast and lung tissues," *IEEE J. Quantum Electron.* **23**(10), 1806–1811 (1987).
5. S. Andersson-Engels et al., "Fluorescence imaging and point measurements of tissue: application to demarcation of malignant tumors and atherosclerotic lesions from normal tissue," *Photochem. Photobiol.* **53**(6), 807–814 (1991).
6. R. Richards-Kortum and E. Sevick-Muraca, "Quantitative optical spectroscopy for tissue diagnosis," *Annu. Rev. Phys. Chem.* **47**, 555–606 (1996).
7. D. C. G. De Veld et al., "The status of *in vivo* autofluorescence spectroscopy and imaging for oral oncology," *Oral Oncol.* **41**(2), 117–131 (2005).
8. D. R. Ingrams et al., "Autofluorescence characteristics of oral mucosa," *Head Neck* **19**(1), 27–32 (1997).
9. A. Gillenwater et al., "Noninvasive diagnosis of oral neoplasia based on fluorescence spectroscopy and native tissue autofluorescence," *Arch. Otolaryngol. Head Neck Surg.* **124**(11), 1251–1258 (1998).
10. D. L. Heintzelman et al., "Optimal excitation wavelengths for *in vivo* detection of oral neoplasia using fluorescence spectroscopy," *Photochem. Photobiol.* **72**(1), 103–113 (2000).
11. D. C. G. De Veldet al., "Autofluorescence characteristics of healthy oral mucosa at different anatomical sites," *Lasers Surg. Med.* **32**(5), 367–376 (2003).
12. M. G. Muller et al., "Spectroscopic detection and evaluation of morphologic and biochemical changes in early human oral carcinoma," *Cancer* **97**(7), 1681–1691 (2003).
13. S. K. Majumder, N. Ghosh, and P. K. Gupta, "Nonlinear pattern recognition for laser induced fluorescence diagnosis of cancer," *Lasers Surg. Med.* **33**(1), 48–56 (2003).
14. B. K. Manjunath et al., "Autofluorescence of oral tissue for optical pathology in oral malignancy," *J. Photochem. Photobiol. B Biol.* **73**(1–2), 49–58 (2004).
15. P. M. Lane et al., "Simple device for the direct visualization of oral-cavity tissue fluorescence," *J. Biomed. Opt.* **11**(2), 024006 (2006).
16. S. D. Kamath and K. K. Mahato, "Optical pathology using oral tissue fluorescence spectra: classification by principal component analysis and k-means nearest neighbor analysis," *J. Biomed. Opt.* **12**(1), 014028 (2007).
17. R. J. Mallia et al., "Laser-induced autofluorescence spectral ratio reference standard for early discrimination of oral cancer," *Cancer* **112**(7), 1503–1512 (2008).
18. J. L. Jayanthi et al., "Discrimination analysis of autofluorescence spectra for classification of oral lesions *in vivo*," *Lasers Surg. Med.* **41**(5), 345–352 (2009).
19. S. Sivabalan et al., "*In vivo* native fluorescence spectroscopy and nicotinamide adinine dinucleotide/flavin adenine dinucleotide reduction and oxidation states of oral submucous fibrosis for chemopreventive drug monitoring," *J. Biomed. Opt.* **15**(1), 017010 (2010).

20. S. N. Shaiju et al., "Habit with killer instincts: *in vivo* analysis on the severity of oral mucosal alterations using autofluorescence spectroscopy," *J. Biomed. Opt.* **16**(8), 087006 (2011).

21. D. C. G. De Veld et al., "Autofluorescence and diffuse reflectance spectroscopy for oral oncology," *Lasers Surg. Med.* **36**(5), 356–364 (2005).

22. N. Subhash et al., "Oral cancer detection using diffused reflectance spectral ratio R540/R575 of oxygenated hemoglobin bands," *J. Biomed. Opt.* **11**(1), 014018 (2006).

23. R. J. Mallia et al., "Oxygenated hemoglobin diffused reflectance for *in vivo* detection of oral pre-cancer ratio," *J. Biomed. Opt.* **13**(4), 014306 (2008).

24. M. Nyberg, K. Ramser, and O. A. Lindhal, "Cancer detection probe combining Raman and resonance sensor technology—experimental study on temperature dependence and effects of molding," *Proc. IFMBE* **25/7**, 331–334 (2009).

25. N. Ramanujam, "Fluorescence spectroscopy *in vivo*," in *Encyclopedia of Analytical Chemistry*, R. A. Meyers, Ed., pp. 20–56, John Wiley & Sons, Chichester (2000).

26. G. A. Wagniers, W. M. Star, and B. C. Wilson, "In-vivo fluorescence spectroscopy and imaging for oncological applications," *Photochem. Photobiol.* **68**(5), 603–632 (1998).

27. Y. Yang et al., "Excitation spectrum of malignant and benign breast tissues: a potential optical biopsy approach," *Lasers Life Sci.* **7**(4), 249–265 (1997).

28. R. Gillies et al., "Fluorescence excitation spectroscopy provides information about skin *in vivo*," *Invest. Dermat.* **115**(4), 704–707 (2000).

29. P. Juzenas et al., "Noninvasive fluorescence excitation spectroscopy during application of 5-aminolevulinic acid *in vivo*," *Photochem. Photobiol Sci.* **1**(10), 745–748 (2002).

30. S. Madhuri et al., "Native fluorescence spectroscopy of blood plasma in the characterization of oral malignancy," *Photochem. Photobiol.* **78**(2), 197–204 (2003).

31. J. Ebenezar, P. Aruna, and S. Ganesan, "Synchronous fluorescence spectroscopy for the detection and characterization of cervical cancers *in vitro*," *Photochem. Photobiol.* **86**(1), 77–86 (2010).

32. P. E. Green and J. Douglas Carroll, *Analyzing Multivariate Data*, Dryden Press, Hinsdale, IL (1978).

33. Y. Yuanlong et al., "Characteristic autofluorescence for cancer diagnosis and its origin," *Lasers Surg. Med.* **7**(6), 528–532 (1987).

34. A. Vannotti, *Porphyrins*, Hilger & Watts Ltd., London (1954).

35. F. N. Ghadially, W. J. P. Neish, and H. C. Dawkins, "Mechanism involved in the production of red fluorescence of human and experimental tumors," *J. Pathol. Bact.* **85**(1), 77–92 (1963).

36. D. M. Haris and J. Werkhaven, "Endogenous porphyrins fluorescence in tumors," *Lasers Surg. Med.* **7**(6), 467–472 (1987).

37. J. K. Dhingra et al., "Early diagnosis of upper aerodigestive tract cancer by autofluorescence," *Arch. Otolaryngol. Head Neck Surg.* **122**(11), 1181–1186 (1996).

38. J. L. Jayanthi et al., "Comparative evaluation of the diagnostic performance of autofluorescence and diffuse reflectance in oral cancer detection: a clinical study," *J. Biophotonics* **4**(10), 696–706 (2011).

39. R. A. Schwarz et al., "Autofluorescence and diffuse reflectance spectroscopy of oral epithelial tissue using a depth-sensitive fiber-optic probe," *Appl. Opt.* **47**(6), 825–834 (2008).

40. P. Diagaradjane et al., "Synchronous fluorescence spectroscopic characterization of DMBA/TPA-induced squamous cell carcinoma," *J. Biomed. Opt.* **11**(1), 014012 (2006).